Structural Study of Langbeinite-type $(NH_4)_2Cd_2(SO_4)_3$ Crystal in the High-temperature Phase

C. MORIYOSHI, E. MAGOME [*], and K. ITOH

Graduate School of Science, Hiroshima University,

Kagamiyama 1-3-1, Higashi-Hiroshima 739-8526, Japan

We determined the crystal structure of the high-temperature cubic phase of the langbeinite-type $(NH_4)_2Cd_2(SO_4)_3$. The observed Cd-O atomic distances are considerably shorter than the standard Cd-O. The structure refinement revealed that the SO_4 ion has several disordered arrangements indicating the existence of the steric hindrance between Cd and SO_4. These results are quite similar to the previously reported characteristics of several $K_2B_2(SO_4)_3$-type langbeinites. We conclude that the steric hindrance between Cd and SO_4 dominates the phase transition, while the NH_4 ion plays no direct role on the phase transition.

RUNNING HEAD: Structural Study of Langbeinite-type $(NH_4)_2Cd_2(SO_4)_3$

INTRODUCTION

Langbeinite-type crystals have the general chemical formula $A_2B_2(SO_4)_3$ (A = K, NH_4, Rb, Tl, Cs; B = Mg, Ni, Zn, Co, Fe, Mn, Ca, Cd).[1] The space group is $P2_13$ in the high-temperature cubic phase. The phase transition is of strong first-order and often displays ferroelectric or ferroelastic activity. The langbeinites exhibit the strange phase transitions such as extremely small critical anomalies of any susceptibilities and a scatter of the reported phase transition temperatures T_t. Therefore, it is difficult to determine the entity of the order parameter, though the phase transition is explained formally by the group theoretical analysis.[2]

---

[*]Present Address : *Faculty of Science, Tokyo University of Science,*

Kagurazaka 1-3, Shinjuku-ku, Tokyo 162-8601, Japan

We performed the accurate X-ray structure analyses of the K-salt langbeinites such as $K_2Mn_2(SO_4)_3$ [3,4], $K_2Co_2(SO_4)_3$ [5], and $K_2Zn_2(SO_4)_3$ [6] in the high-temperature cubic phase to reveal the following strange characteristics common to these crystals. (1) The *B*-O distances, $d_{B\text{-}O}$, of the average structure (*B* = Mn, Co and Zn) are considerably shorter than the standard ones. (2) The SO_4 ion has the multi-site disordered arrangements. (3) Mean-square atomic displacements of all the constituent atoms increase with approaching T_t in the cubic phase, though no mode softening has been found. (4) The extinction effect of X-ray diffraction lessens with approaching T_t. (5) A discrepancy factor of the structure analysis becomes large with approaching T_t. (6) We often find that T_t depends on samples or experiments. We have explained these results by the nucleation and growth type phase transition model in which the steric hindrance between the *B* ions and the surrounding SO_4 ions is assumed to be a driving force of the phase transition. This model is supported by the neutron powder diffraction study [7] and micro-Raman studies [8-10] of $K_2Mn_2(SO_4)_3$. In the neutron diffraction patterns, the coexistence of the peaks of the high- and low-temperature phases has been observed in the relatively wide temperature range.[7] By the micro-Raman studies of $K_2Mn_2(SO_4)_3$, it has been revealed that T_t varies with the position of the sample in the temperature range about 7 K.[8-10] The neutron diffraction study has also clarified that most of $d_{Mn\text{-}O}$'s are larger in the low-temperature phase than in the high-temperature phase, contrary to the fact that the unit cell volume becomes smaller in the low-temperature phase.[7] This result indicates that the steric hindrance in the high-temperature phase is relaxed in the low-temperature phase. Recently, clarifying the role of two independent *B*-sites, *B*(1) and *B*(2), we studied the cubic crystal structure and its annealing effect of the $K_2Cd_{2c}Mn_{2(1-c)}(SO_4)_3$ mixed crystal (nominally $c = 0.5$).[11,12] The Cd concentrations of the unannealed crystal are $c_1 < c$ for the *B*(1)-site which forms the short $d_{Cd/Mn(1)\text{-}O}$ against $c_2 \cong c$ for the *B*(2)-site, and both c_1 and c_2, in particular c_1, are reduced by annealing. This

concentration analysis has established the existence of the steric hindrance around two kinds of the *B*-sites, in particular around the *B*(1)-site, because small *c* means that the larger Cd ion is difficult to occupy the site where the strong steric hindrance exists. It was clarified for the K-salt langbeinites that 'the strength of the steric hindrance' *S* of the *B*(1)-site can be expressed by $S \sim aT_t + b$, where *a* and *b* are positive constants. Therefore, we have concluded that the phase transition of the K-salt langbeinites is commonly dominated by the steric hindrance between the *B* ions, especially *B*(1), and the surrounding SO_4 ions.

It is of interest whether the phase transition of not the K-salts ($A \neq K$) can also be explained by this scheme. In this study, we notice the ferroelectric $(NH_4)_2Cd_2(SO_4)_3$ (abbreviated to ACS) because the NH_4 ion has an anisotropic electron distribution in contrast to the K ion. ACS undergoes a first-order phase transition from the high-temperature cubic phase ($P2_13$) to the low-temperature monoclinic phase ($P2_1$). The ferroelectricity of ACS was found by Jona and Pepinsky.[13] Raman, infrared and far-infrared studies have found no mode softening and suggested the disordering of the SO_4 ion in the high-temperature phase.[14] Proton NMR and EPR studies have reported that the NH_4 ion as well as the SO_4 ion has dynamical disordered arrangements.[15-18] Anomaly of the dielectric constant is unobserved even just above T_t.[19] The reported T_t is scattered from 89 to 95 K.[13,15,16,19,20] Some additional anomalies of the heat capacity are observed near T_t to suggest that the crystal is inhomogeneous.[20] The micro-Raman study shows that T_t distributes in a sample from 88 to 90 K to indicate the existence of the nuclei with the micron scale.[9] These results suggest that the phase transition scheme of ACS resembles that of the K-salts. Unfortunately, the crystal structure of pure ACS has not been determined yet, although that of $(NH_4)_2Cd_{0.84}Mn_{1.16}(SO_4)_3$ mixed crystal is known.[21]

The purpose of this study is to determine the high-temperature structure of ACS with special attention to the Cd-O distances and the behavior of the SO_4 ions which are the key of the

above mentioned steric hindrance scheme. We discuss the phase transition mechanism of ACS by comparing with the well established one of the K-salt langbeinites.

EXPERIMENTAL

Single crystals of ACS were grown from an aqueous solution of $(NH_4)_2SO_4$ and $CdSO_4 \cdot nH_2O$ ($n \sim 8/3$) by the evaporation method. A fragment cut out from a parent crystal was polished with sandpaper to a sphere whose diameter is $2r = 0.51(1)$ mm. We dipped the sample crystal into liquid nitrogen several times to reduce an extinction effect. X-ray diffraction intensities were measured at $T = 301$ K using an automatic four-circle diffractometer Rigaku AFC-5R with graphite-monochromated MoKα radiation up to $2\theta = 127°$ with the scanning rate 2°/min. in the θ-2θ scanning mode. The space group of the high-temperature cubic phase was confirmed to be $P2_13$ from the systematic absences of the diffraction intensities. The cubic lattice parameter is $a = 10.350(4)$ Å.

For the crystal structure analysis, we used 3294 diffraction intensities satisfying the condition $|F_o| \geq 3\sigma(|F_o|)$, where $\sigma(|F_o|)$ is the estimated standard deviation of the absolute value of the structure factor F_o. An absorption correction of X-rays ($\mu r = 1.13$) and a correction of the anomalous scattering effect were made for Cd, S, O and N atoms. We refined the structure using the full-matrix least squares program RADIEL taking an isotropic secondary extinction effect into account.[22] The function minimized in the least squares calculation is $R_w = \left\{\sum w(H)(|F_o(H)| - |F_c(H)|)^2 / \sum w(H)|F_o(H)|^2\right\}$, where $w(H) = 1/\sigma^2(F_o(|H|))$. We adopted the same crystal axes as selected in the K-salts [3-7,11,12] instead of those used in the previous mixed crystal study.[21] The structural parameters of $K_2Mn_2(SO_4)_3$ [3] were used as starting parameters of the least squares calculation. Since the symmetry constraint was not appropriate in the mixed crystal study [21], we considered correctly the constraint of the site symmetry 3 for the Cd and N positions. We tried to determine the positions of the H

atoms from a difference Fourier map but found no significant peaks as mentioned in the next section.

RESULTS

The atomic parameters of the non-hydrogen atoms were determined on the basis of the average structure model. The discrepancy factor is R_w = 0.0246. The positional and thermal parameters of the average structure are listed in Table 1. This average structure is quite similar to the K-salts. As for the H atoms, the difference Fourier map around the N atoms shows only the residual electron density less than 0.1 e/Å^3 which is nearly equal to the background value. This result strongly suggests that the NH_4 ions take a disordered arrangement as has been reported by the NMR and EPR studies.[15-18] The standard deviations of the atomic parameters are less than one third of those of the previous mixed crystal study [21], so that the present structure is determined accurately to discuss the

TABLE 1. Positional parameters x, y, z (fraction) and thermal parameters U_{ij} (10^{-2} Å^2) in the high-temperature cubic phase of ACS at T = 301 K. Anisotropic temperature factor is defined by $\exp[-2\pi^2(h^2a^{*2}U_{11} + k^2b^{*2}U_{22} + l^2c^{*2}U_{33} + 2hka^*b^*U_{12} + 2hla^*c^*U_{13} + 2klb^*c^*U_{23})]$. For the Cd and N atoms, $x = y = z$, $U_{11} = U_{22} = U_{33}$ and $U_{12} = U_{13} = U_{23}$.

Atom	x	y	z	U_{11}	U_{22}	U_{33}	U_{12}	U_{13}	U_{23}
Cd(1)	0.33053(4)	0.33053	0.33053	1.35(1)	1.35	1.35	-0.08(1)	-0.08	-0.08
Cd(2)	0.58687(4)	0.58687	0.58687	1.35(1)	1.35	1.35	-0.09(1)	-0.09	-0.09
N(1)	0.8154(5)	0.8154	0.8154	2.2(2)	2.2	2.2	0.0(2)	0.0	0.0
N(2)	0.0506(6)	0.0506	0.0506	2.5(2)	2.5	2.5	-0.1(2)	-0.1	-0.1
S	0.22453(4)	0.37527(4)	0.01019(4)	1.06(1)	1.05(1)	1.13(1)	0.19(1)	-0.04(1)	0.06(1)
O(1)	0.3124(2)	0.2753(2)	0.9652(2)	2.43(8)	2.33(8)	5.06(12)	1.18(6)	0.25(8)	-1.02(8)
O(2)	0.0916(2)	0.3285(2)	-0.0044(2)	1.29(5)	3.52(8)	4.15(9)	-0.70(6)	0.38(6)	-1.67(8)
O(3)	0.2463(2)	0.4909(2)	0.9332(2)	4.91(11)	2.53(8)	3.59(10)	0.33(8)	0.30(10)	2.00(8)
O(4)	0.2487(2)	0.4087(2)	0.1454(2)	4.65(10)	3.54(9)	1.70(6)	0.26(10)	-1.27(7)	-0.44(7)

structural details. Figure 1 is the average structure of ACS, where the anisotropic thermal vibrations are drawn by the 50% probability ellipsoid. All the thermal vibrations of the O atoms are large and highly anisotropic, while those of the N, Cd and S atoms are much smaller than those of the O atoms and more isotropic.

We tabulate the atomic distances between the Cd and O atoms, $d_{Cd\text{-}O}$, and between the N and O atoms, $d_{N\text{-}O}$, and the bond lengths and angles of the tetrahedral SO_4 ion in Table 2. It should be noticed that $d_{Cd\text{-}O}$'s in the range from 2.246(2) to 2.276(2) Å are quite shorter than the standard value $d^0_{Cd\text{-}O}$ = 2.346 Å.[23] This result indicates that, as is expected from the K-salts, there exists the steric hindrance between the Cd and SO_4 ions. On the other hand, the observed $d_{N\text{-}O}$'s lie in the range of the normal hydrogen bond lengths $d^0_{N\text{-}O}$ which are in the range 2.73 to 3.22 Å.[23] We can also see that the shape of the SO_4 ion is rather regular and $d_{S\text{-}O}$'s are

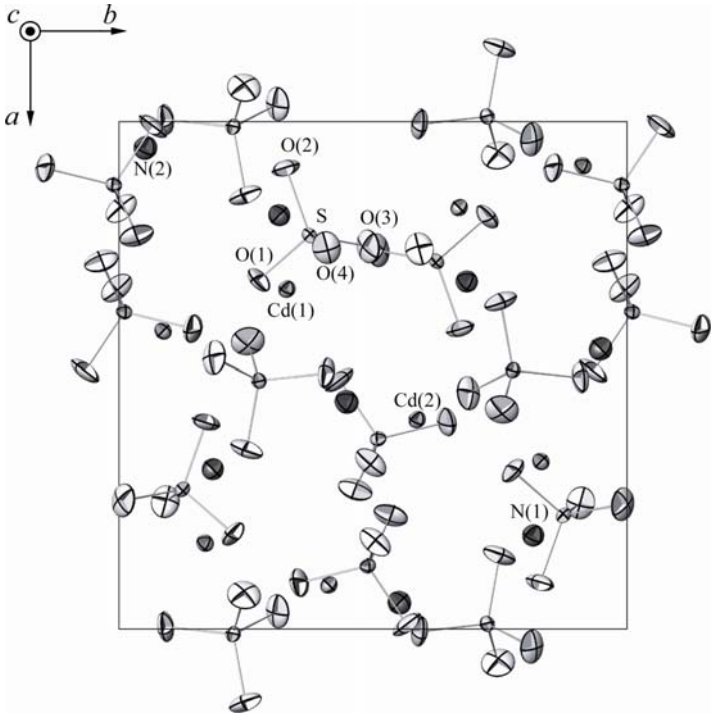

FIGURE 1. The average structure of ACS in the high-temperature cubic phase (T = 301 K). The atoms attached by the chemical symbols are the structurally independent atoms, of which parameters are given in Table 1. Thermal vibrations are depicted by the 50% probability ellipsoid.

TABLE 2. Nearest-neighbor metal-oxygen distances (Å), and bond lengths (Å) and angles (º) of the SO_4 tetrahedron calculated from the average structure.

Cd(1)	–	O(3)	2.275(2)	S	–	O(1)		1.455(2)
Cd(1)	–	O(4)	2.246(2)	S	–	O(2)		1.466(2)
Cd(2)	–	O(1)	2.276(2)	S	–	O(3)		1.455(2)
Cd(2)	–	O(2)	2.252(2)	S	–	O(4)		1.463(2)
N(1)	–	O(1)	3.218(6)	O(1)	–	S	– O(2)	108.6(1)
N(1)	–	O(3)	3.214(6)	O(1)	–	S	– O(3)	108.3(1)
N(1)	–	O(4)	2.966(6)	O(1)	–	S	– O(4)	111.6(1)
N(2)	–	O(1)	3.058(7)	O(2)	–	S	– O(3)	111.1(1)
N(2)	–	O(2)	2.962(7)	O(2)	–	S	– O(4)	109.7(1)
N(2)	–	O(3)	3.184(7)	O(3)	–	S	– O(4)	107.6(1)

almost lower limit of the standard bond length. This is due to large thermal vibrations of the O atoms.

Clarifying the disordered characteristics of the SO_4 ion, we analyzed the multi-site disorder model of SO_4 by using the split-atom method based on the n-site O atom model ($n \leq 10$) in the same way as the previous studies.[4-6,12] We assumed the thermal vibrations of the O atoms are anisotropic for $1 \leq n \leq 4$ and isotropic for $5 \leq n \leq 10$. The occupation probability of each disordered site is assumed to be $1/n$. Table 3 shows R_w of these disorder models. On the basis of the Hamilton's significance test [24], the 4-site anisotropic disorder model is most probable. We depict the 4-site disordered SO_4 ion along with the 50% probability thermal ellipsoid of the average structure in Figure 2. The disordered O atom positions (filled circle) are distributed within the ellipsoid of the average positions. Here, as we have emphasized in the preceding studies [4-6,12], it should be said that the split 4-site positions would not correspond directly to the true equilibrium sites but give the probability density function of the O atoms as a whole. This is because that the multi-site disorder includes not only the dynamical character clarified by the Raman and other studies but also the static one due to the structural inhomogeneity. We conclude that the disordering of the SO_4 ion induced by the

steric hindrance between the Cd and SO_4 ions exists in ACS, as has been clarified in the K-salts.

TABLE 3. Discrepancy factor R_w of the average structure model (n = 1) and the multi-site disorder models (n = 2 ~ 10). The n = 4 model is most probable.

n	number of parameters	R_w	thermal vibration model
1	59	0.0246	anisotropic
2	95	0.0220	
3	131	0.0215	
4	167	0.0212	
5	103	0.0222	isotropic
6	119	0.0218	
7	135	0.0216	
8	151	0.0215	
9	167	0.0214	
10	183	0.0213	

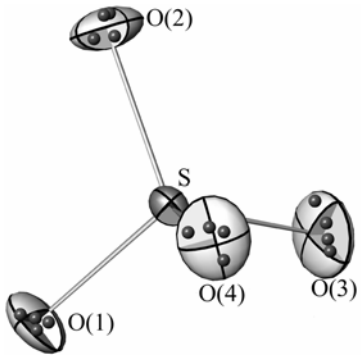

FIGURE 2. The disordered arrangement of the SO_4 tetrahedron. Filled circles stand for the split O atom positions. Thermal vibrations of the average structure model are superimposed with the ellipsoid of 50% probability. This disordering is induced by the steric hindrance between the Cd and SO_4 ion.

DISCUSSION

The structural characteristics revealed in ACS such as the short Cd-O distances and the multi-site disordering of SO_4 are the same as observed in the K-salt langbeinites. Therefore, the

phase transition of ACS can also be described by the steric hindrance scheme proposed for the K-salts. At $T_t < T$, the short $d_{Cd(1)-O}$ along with $d_{Cd(2)-O}$ causes the steric hindrance between the Cd and the neighboring SO_4 ions to induce the multi-site disordering of SO_4. The steric hindrance grows with approaching T_t from above, and the phase transition takes place by resolving the steric hindrance to cause the ordering of the SO_4 ion below T_t. In ACS, the ordering of the NH_4 ion is induced by the SO_4 ordering via the hydrogen bond N-H···O. It is reasonable to think that the NH_4 ion in ACS has no direct role in the phase transition as the K ion is so in the K-salts.

It is of interest to evaluate the strength of the steric hindrance $S(i)$ (i = 1, 2) [12] between the $B(i)$ and SO_4 ions defined by

$$S(i) = -\left(d_{B(i)-O} - d^0_{B-O}\right)/ d^0_{B-O}\,. \qquad (1)$$

The steric hindrance exists when $S > 0$ and the strength develops with increasing S. Noticing the shorter $d_{B(1)-O}$, we have evaluated that $S(1) = 0.013 \sim 0.045$ for the K-salts.[12] In the case of ACS, inserting $d_{Cd(1)-O} = 2.261$ Å, which is the average of $d_{Cd(1)-O(3)}$ and $d_{Cd(1)-O(4)}$, and the standard distance $d^0_{Cd-O} = 2.346$ Å into eq. (1), we obtain $S(1) = 0.036$. Therefore, we are convinced that the steric hindrance scheme is also valid for ACS. Here, let us compare $S(1)$ of ACS with that of $K_2Cd_2(SO_4)_3$. We find that $S(1) = 0.036$ of ACS ($T_t \sim 90$ K) is smaller than $S(1) = 0.045$ of $K_2Cd_2(SO_4)_3$ ($T_t = 432$ K [25]).[12] This result is consistent with the above mentioned empirical relation $S \sim aT_t + b$ ($S \sim (T_t + 100) \times 10^{-4}$ for the K-salts [12]), though slight deviation of S of ACS from this straight line is seen, to suggest strongly that the phase transition of ACS is also driven by the steric hindrance between the B and SO_4 ions. In connection with this deviation, we should notice that $S(2) = 0.035$ for ACS. The relation $S(1) \sim S(2)$ is characteristic of ACS because $S(1) > S(2)$ always holds for the K-salts. It seems that this minor structural difference will be related to the deviation of S of ACS from the straight line determined from the K-salts.

Finally we comment on the small anomaly of any kind of susceptibility χ of ACS. First, the phase transition of ACS is inherently of strong first-order. In addition to this, it seems that the nucleation and growth mechanism suppresses the increase of χ. According to the Ornstein Zernike equation [26], the correlation length ξ_c is expressed by

$$\xi_c \propto \left(\frac{T}{T - T_t} \right)^{1/2}. \qquad (2)$$

If a system is homogeneous, χ diverges at $T = T_t$, because ξ_c diverges at $T = T_t$. On the other hand, in the inhomogeneous nucleation and growth system, χ remains finite even at $T \sim T_t$, because ξ_c is less than the nucleus size L, which is estimated to be of the order of micron even at $T \sim T_t$ from the observation of Bragg diffraction and the site dependence of T_t by the micro-Raman studies.[8-10]

ACKNOWLEDGEMENT

The authors thank Foundation for Promotion of Material Science and Technology of Japan (MST Foundation) for the financial support.

REFERENCES

[1] Hellwege K.-H. and Hellwege A.M. ed. Landolt-Börnstein, Ⅲ/16b. Berlin, Heidelberg, New York: Springer-Verlag (1982).

[2] Dvořák V.: Structural phase transitions in langbeinites. Phys. Status Solidi B **52**, 93-98 (1972).

[3] Ukeda T., Itoh K., and Moriyoshi C.: Structural study of phase transition in langbeinite-type $K_2Mn_2(SO_4)_3$ crystals. J. Phys. Soc. Jpn. **64**, 504-512 (1995).

[4] Moriyoshi C. and Itoh K.: Multi-site disordering of SO_4 ion of langbeinite-type $K_2Mn_2(SO_4)_3$ crystal in the cubic phase. J. Phys. Soc. Jpn. **65**, 3082-3083 (1996).

[5] Moriyoshi C., Itoh K., and Hikita T.: Structural study of phase transition in $K_2Co_2(SO_4)_3$ crystals. J. Phys. Soc. Jpn. **64**, 4726-4732 (1995).

[6] Moriyoshi C. and Itoh K.: Structural study of phase transition mechanism of langbeinite-type $K_2Zn_2(SO_4)_3$ crystals. J. Phys. Soc. Jpn. **65**, 3537-3543 (1996).

[7] Dilanian R.A., Izumi F., Itoh K., and Kamiyama T.: Neutron powder diffraction study of the order-disorder transition in $K_2Mn_2(SO_4)_3$. J. Phys. Soc. Jpn. **68**, 3893-3900 (1999).

[8] Sakai A., Kitoh M., Negishi M., and Itoh K.: Micro-Raman scattering study of the phase transition of $K_2Mn_2(SO_4)_3$. Ferroelectrics **217**, 99-103 (1998).

[9] Sakai A., Negishi M., Fujiwara E., Moriyoshi C., and Itoh K.: Micro-Raman spectra of langbeinite-type $K_2Mn_2(SO_4)_3$ and $(NH_4)_2Cd_2(SO_4)_3$ near the phase transition temperature. J. Phys. Soc. Jpn. **70**, 3452-3456 (2001).

[10] Sakai A., Inagaki T., Moriyoshi C., and Itoh K.: Micro-Raman mapping study of the phase transition in $K_2Mn_2(SO_4)_3$. Ferroelectrics **272,** 27-32 (2002).

[11] Magome E., Moriyoshi C., Itoh K., and Vlokh R.: X-ray structure analysis of $K_2Cd_{2x}Mn_{2(1-x)}(SO_4)_3$ mixed crystal in the high-temperature phase. Ferroelectrics **269**, 93-98 (2002).

[12] Magome E., Itoh K., Moriyoshi C., and Vlokh R.: Steric hindrance in langbeinite-type $K_2Cd_{2c}Mn_{2(1-c)}(SO_4)_3$ mixed crystal. J. Phys. Soc. Jpn. **73**, 2444-2448 (2004).

[13] Jona F. and Pepinsky R.: Ferroelectricity in the langbeinite system. Phys. Rev. **103**, 1126 (1956).

[14] Kreske S. and Devarajan V.: Vibrational spectra and phase transitions in ferroelectric-ferroelastic langbeinites: $K_2Mn_2(SO_4)_3$, $(NH_4)_2Cd_2(SO_4)_3$ and $Tl_2Cd_2(SO_4)_3$. J. Phys. C **15**, 7333-7350 (1982).

[15] McDowell C.A., Raghunathan P., and Srinivasan R.: Proton N.M.R. study the dynamics of the ammonium ion in ferroelectric langbeinite $(NH_4)_2Cd_2(SO_4)_3$. Mol. Phys. **29**, 815-824 (1975).

[16] Misra S.K. and Korczak S.Z.: Mn^{2+} EPR study of the phase transition in langbeinite $Cd_2(NH_4)_2(SO_4)_3$. J. Phys. C **19**, 4353-4361 (1986).

[17] Babu D.S., Sastry G.S., Sastry M.D., and Dalvi A.G.I.: EPR study of structural phase transitions in $(NH_4)_2Cd_2(SO_4)_3$. Phase Transitions **15**, 11-20 (1989).

[18] Babu D.S., Sastry G.S., Sastry M.D., and Dalvi A.G.I.: Structural phase transitions in langbeinites: an EPR study. J. Phys. C **17**, 4245-4253 (1984).

[19] Ohshima H. and Nakamura E.: Dielectric properties of ferroelectric $(NH_4)_2SO_4$, $(NH_4)_2BeF_4$ and $(NH_4)_2Cd_2(SO_4)_3$ at 10 *kc/s*. and 3.3 *kMc/s*. J. Phys. Chem. Solids **27**, 481-486 (1966).

[20] Artman J.I. and Boerio-Goates J.: Heat capacity studies of phase transitions in langbeinites III. Ferroelectrics **132**, 141-152 (1992).

[21] Ng H.N. and Calvo C.: Crystal structure of and electron paramagnetic resonance of Mn^{2+} in $Cd_2(NH_4)_2(SO_4)_3$. Can. J. Chem. **53**, 1449-1455 (1975).

[22] Coppens P., Guru Row T.N., Leung P., Stevens E.D., Becker P.J., and Yang Y.W.: Net atomic charges and molecular dipole moments from spherical-atom X-ray refinements, and the relation between atomic charge and shape. Acta Crystallogr. Sect. A **35**, 63-72 (1979).

[23] Henry N.F.M. and Lonsdale K. ed. International Tables for X-ray Crystallography, III. Birmingham: Kynoch Press (1969), p. 261, 273.

[24] Hamilton W.C.: Significance tests on the crystallographic *R* factor. Acta Crystallogr. **18**, 502-510 (1965).

[25] Lissalde F., Abrahams S.C., Bernstein J.L., and Nassau K.: X-ray diffraction and dielectric temperature dependence study of the $K_2Cd_2(SO_4)_3$ paraelastic-ferroelastic phase transition. J. Appl. Phys. **50**, 845-851 (1979).

[26] Brout R.: Phase transitions. New York: W. A. Benjamin, Inc. (1969), Chap. 2.